ISSN 0869-5938, Stratigraphy and Geological Correlation, 2025, Vol. 33, No. 5, pp. 591–608. © Pleiades Publishing, Ltd., 2025.

U–Th–Pb (LA-ICP-MS) Dating of Detrital Zircons from Jurassic Deposits of the Franz Josef Land Archipelago (Russian Arctic) and the Evolution of Their Provenance

Yu. V. Karyakin[a, *], V. B. Ershova[a, b], G. N. Aleksandrova[a, **], S. M. Lyapunov[a], A. S. Dubenskiy[a], S. Yu. Sokolov[a], N. P. Chamov[a], K. G. Erofeeva[a, c], and V. S. Sheshukov[a]

[a] *Geological Institute, Russian Academy of Sciences, Moscow, 119017 Russia*
[b] *St. Petersburg State University, St. Petersburg, 199034 Russia*
[c] *Institute of Ore Geology, Petrography, Mineralogy, and Geochemistry, Russian Academy of Sciences, Moscow, 119017 Russia*
**e-mail: yukar61@mail.ru*
***e-mail: dinoflag@mail.ru*

Received December 30, 2024; revised February 26, 2025; accepted March 28, 2025

Abstract—We present the results of U–Pb dating of detrital zircon from Lower to Middle Jurassic sedimentary rocks, sampled from natural outcrops during fieldwork on Hooker, Hayes, Ziegler, Jackson, and Graham Bell islands of the Franz Josef Land archipelago. Considering the geographic distribution of the studied samples, we characterize the spatial distribution of detrital zircon ages from Early Jurassic (Pliensbachian) and Middle Jurassic (Bajocian–Bathonian) strata across the archipelago. Based on this, we reconstruct the evolution of sediment source areas in both time and space. The data show that during the Pliensbachian and Bajocian, the main provenance areas were uplifts composed of metamorphic (Meso- to Neoproterozoic), magmatic (Cambrian and Late Devonian–Carboniferous), and Cambrian–Triassic sedimentary rocks, which were exposed during Late Triassic to Early Jurassic uplift in the northeastern Barents Sea region. By the Bajocian–Bathonian boundary, most of these uplifts had been significantly eroded. A major transgression, initiated in the Toarcian, culminated at the end of the Bajocian, leading to an expansion of marine sedimentation and a substantial reduction in the extent of continental landmasses. The dominant sediment sources at that time were likely limited to small land areas composed of Permian and/or Lower to Middle Triassic strata.

Keywords: Arctic islands of Russia, isotopic age, Early Jurassic, Middle Jurassic, Toarcian, Bajocian–Bathonian

DOI: 10.1134/S0869593825700261

INTRODUCTION

The marginal-shelf arch of the Franz Josef Land (FJL) Archipelago formed as a structural unit in the extreme north of the Barents Sea continental margin at the beginning of the Mesozoic. In the north, the uplift borders the deep-water Nansen Basin, which is part of the Eurasian Basin. In the south, the archipelago borders the North and East Barents basins. To the west and east, it is surrounded by the rift-related Franz Victoria and St. Anna depressions (Gramberg, 1988).

In the sedimentary history of the Barents Sea continental margin, two major transgressive–regressive cycles are distinguished: the Triassic and the Early Jurassic to Early Cretaceous cycles (Preobrazhenskaya et al., 1985; Gramberg, 1988; Basov et al., 1997, 2009). The Triassic cycle began with a marine transgression in the Induan, included several second-order regressive episodes, and terminated with a general regression at the end of the Triassic. On FJL, the oldest Triassic (Induan?) terrigenous sedimentary deposits overlie Upper Carboniferous limestones transgressively. These deposits were penetrated by the Nagursky parametric borehole on Alexandra Land (Gramberg et al, 1985; Dibner, 1998). In two other boreholes (Hayes borehole, Hayes Island, and Severnaya borehole, Graham Bell Island), the Triassic section includes all stratigraphic subdivisions of middle and upper series except for the Rhaetian. On the basis of lithological and facies data, it has been suggested that the detrital material in the Triassic may have been supplied to the FJL area from the Severnaya Zemlya and Svalbard archipelagos, as well as from the Novaya Zemlya–Urals region and Baltica (Pchelina, 1998; Basov et al., 2009).

The Early Jurassic–Early Cretaceous cycle of sedimentation coincides chronologically with a significant rearrangement of the geodynamic regime in the Arctic region—the formation of the heterogenous structure of the Amerasia Basin. This process began with rifting in the Canadian Basin in the Early–Middle Jurassic (for example, Grantz et al., 1998; Mickey

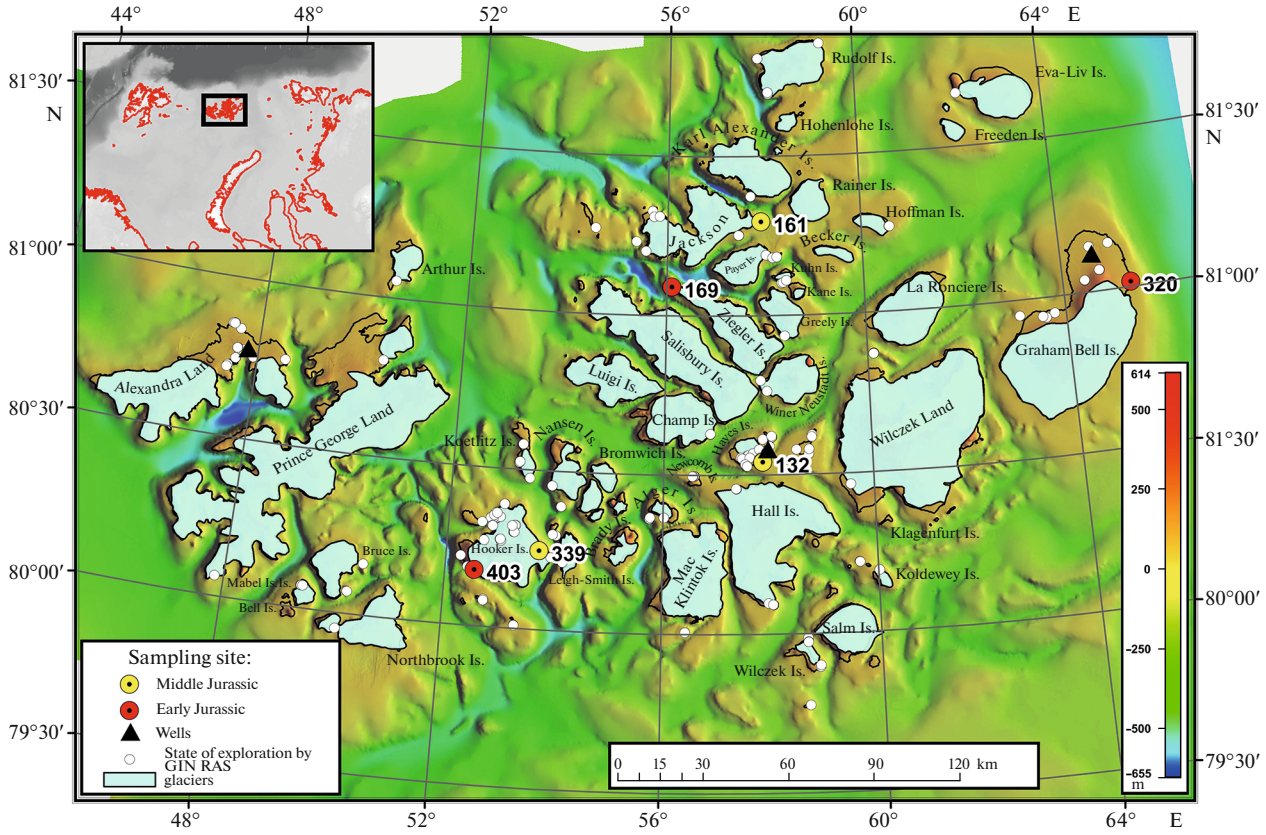

Fig. 1. Schematic geographical map of the Franz Josef Land (FJL) Archipelago, indicating sampling sites for U–Pb dating of detrital zircons.

et al., 2002; Grantz, 2006). The onset of the cycle in the Barents Sea region is characterized by the accumulation of sedimentary deposits of continental origin (Gramberg, 1988). Within the FJL, these are Early Jurassic quartz sands and sandstones of the Tegethoff Formation (Dibner and Sedova, 1959; Dibner, 1998). The marine transgression that began in the Aalenian, initially covering only the islands of the western and central parts of the archipelago, terminated with a general regression during the Berriasian–Aptian interval (Basov et al., 2009). Clayey and silty-clayey deposits rich in marine fauna were accumulated during the Bajocian and Bathonian stages (Fiuma Formation after (Kosteva, 2002, 2005)). The transgression reached its maximum extent in the Callovian. Lithofacies analysis suggests that the main sediment source areas during the Jurassic were located to the north and northeast of the archipelago (Kosteva, 2002).

For the Mesozoic deposits of the FJL, U–Pb (LA-ICP-MS), dating of detrital zircons from Middle–Upper Triassic terrigenous deposits penetrated by the Severnaya borehole (Soloviev et al., 2015) and Upper Triassic–Cretaceous deposits from the southeastern islands of the FJL (Ershova et al., 2022) was conducted previously. According to Soloviev et al. (2015), detrital material was supplied to the Middle–Late Triassic basin from the southeast and east, with the mountain structures of the Ural fold belt and, to a lesser extent, the East European craton and Timanides serving as the sources of clastic material. Ershova et al. (2022) proposed that the provenance area for Late Triassic–Early Jurassic deposits was near FJL and represented an extension of the Taimyr branch of the Uralian orogen, which underwent significant uplift at the end of the Triassic.

We have studied Lower–Middle Jurassic terrigenous deposits, samples of which were collected in the north (Ziegler Island, Jackson Island), central (Hooker Island, Hayes Island), and east (Graham Bell Island) parts of the FJL archipelago (Fig. 1). For all Jurassic outcrops studied—except for Graham Bell Island—U–Pb dating of detrital zircons is conducted here for the first time. The first provenance reconstruction based on detrital zircons from Jurassic strata of Franz Josef Land (Ershova et al., 2022) was based solely on samples collected from the southeastern part of the archipelago. The aim of our study is to provide a more comprehensive understanding of sediment source areas and the paleogeography of the region during the Early and Middle Jurassic.

OBJECTS OF INVESTIGATION

Jurassic sedimentary deposits in the FJL area are undisturbed and gently dipping. The fragmentary

nature of the outcrops, combined with the large lithological variability at each stratigraphic level and variation in thickness, greatly complicates their correlation across the archipelago. This accounts for the absence of a universally accepted stratigraphic framework for the Jurassic deposits of the Franz Josef Land Archipelago. As a result, these deposits are typically subdivided using biostratigraphic methods, with different researchers proposing regionally significant units—such as series, formations, and members—that vary in extent and composition (Dibner and Sedova, 1959; Dibner, 1998; Kosteva, 2002, 2005; Repin et al., 2007). Accordingly, the age of the studied samples is determined based both on published data regarding the age of the Jurassic sedimentary rocks of the archipelago, and on our own palynological analyses where such data are lacking. In our research, we used the stratigraphic scheme (Fig. 2) proposed by Kosteva (2002), which was supplemented with recent data from other studies (Stolbov et al., 2010; Khudoley et al., 2019; Karyakin et al., 2021; Ershova et al., 2022; Karyakin and Aleksandrova, 2023). According to these data, the Fiume Formation is composed not only of clays and mudstones (the stratotype is located at Cape Fiume, Champ Island) but also of coeval sands and sandstones. The facies transition to the latter is recorded, in particular, in the eastern part of Hooker Island, between Solnechnaya Rock and the outcrop at an elevation of 371 m. These sands continue further to the south, to outcrop 339 (Fig. 1), and even further south to the Makarov Bay area. According to available data, the Fiume Formation is composed not only of claystones and argillites, as observed in its type section at Cape Fiume on Champ Island, but also of coeval sands and sandstones. A direct facies transition between these lithotypes is observed, in particular, in the eastern part of Hooker Island, between Solnechnaya Rock and the outcrop at an elevation of 371 m. These sands can be traced further south to outcrop 339 (Fig. 1), and even farther into the Makarov Bay area. In the western part of Franz Josef Land, the Fiume Formation is stratigraphically equivalent to Bajocian–Bathonian sands exposed at Cape Stephens on George Land Island (Stolbov et al., 2004). In the central and northern parts of the archipelago, the same stratigraphic interval is represented by Bathonian sands, sandstones, and argillites on Hayes and Jackson islands (outcrops 132 and 161, Fig. 1).

The Lower Jurassic deposits belong to the Tegethoff Formation, which was identified as a stratigraphic unit by V.D. Dibner (Dibner, 1957; Dibner and Sedova, 1959). These sedimentary rocks, which contain Early Jurassic (Pliensbachian) palynocomplexes and are among the most common in the FJL, were identified on many islands of the archipelago, from Bell Island in the southwest to Graham Bell Island in the northeast (Kosteva, 2002, 2005; Repin et al., 2007). On Leigh-Smith Island, the stratigraphic interval of the Tegethoff Formation has been extended to Pliensbachian–Toarcian on the basis of new data (Karyakin and Aleksandrova, 2023).

In our collection, these deposits are represented by sands and sandstones of Hooker, Ziegler, and Graham Bell islands (Figs. 1, 2).

On Hooker Island (80°10′33.9″ N, 52°32′56.7″ E), in the Lunacharsky Rock area (outcrop 403, Sample 403-1; Figs. 3a, 3b), samples were collected from a unit of massive, fine- and medium-grained arkosic sands. These sands consist of plagioclase, quartz, mica, hornblende, and lithic fragments, as well as an insignificant amount of ore minerals. The sandstones contain interbeds enriched in coaly material, lenses of siliceous–quartz gravelstones, marcasite concretions, and fragments of mineralized and coalified wood. The unit underlies the basalt nappe that is believed to be of Early Jurassic age. The sands contain a Pliensbachian palynological assemblage, as well as dinocysts (Karyakin and Aleksandrova, 2023). It should be noted that these sands also contain redeposited Triassic pollen and spores (*Aratrisporites* sp., *Lunatisporites* spp., *Riccisporites* sp., etc.) (Karyakin and Aleksandrova, 2023).

On Ziegler Island (outcrop 169, Sample 169-3; Figs. 3c, 3d), in the Cape Brice area (81°05′23.5″ N, 56°06′23.0″ E), samples were collected from massive and platy arkosic sandstones, locally enriched in carbonaceous matter. The sandstones with an apparent thickness of 3.5–4 m are overlain by a volcani-clastic unit, consisting of several Early Cretaceous basaltic lava flows that are intruded by Early Cretaceous dikes of subalkaline basalts (Karyakin and Sokolov, 2018; Karyakin et al., 2021). On Cape Kohlsaat on Graham Bell Island (81°00′55.8″ N, 65°21′49.5″ E), a light gray essentially siliceous-quartz sands of Pliensbachian age was sampled (outcrop 320, Sample 320; Figs. 3e, 3f), which crop out on the northeastern slope of Mount Kohlsaat (Kosteva, 2002).

Middle Jurassic deposits are represented by samples collected from sand and sandstone units that are exposed only fragmentarily on Hooker, Hayes, and Jackson islands (Figs. 1, 2).

On Hooker Island, in the outcrop, located 5 km to the northwest from Cape Al'banova (80°14′55.8″ N, 53°42′44.3″ E), the fine-grained light gray quartz and feldspar-quartz sands enclosing thin interbeds of carbonaceous matter (outcrop 339, Sample 339) was sampled (Figs. 4a, 4b). The apparent thickness is 17–18 m. Sands underlie a series of flows of Early Cretaceous tholeiitic basalts with a well-pronounced (25–30 cm) contact zone (Fig. 4b).

Sample 339 contains a diverse palynological complex, with a predominance of spores of different systematics. *Cyathidites minor*, *C.* spp., and *C. australis* dominate. *Stereisporites kemtchygiensis*, *S. psilatus*, *S. insertus*, *Marattisporites scabratus*, *Neoraistrickia truncata*, *N. rotundiformis*, *N. longibaculata*, *Osmundacidites* spp., and *Dictyophyllidites harrissii* are common. There are also single *Todisporites* sp., *Biretisporites* sp., *Cibotiumspora*

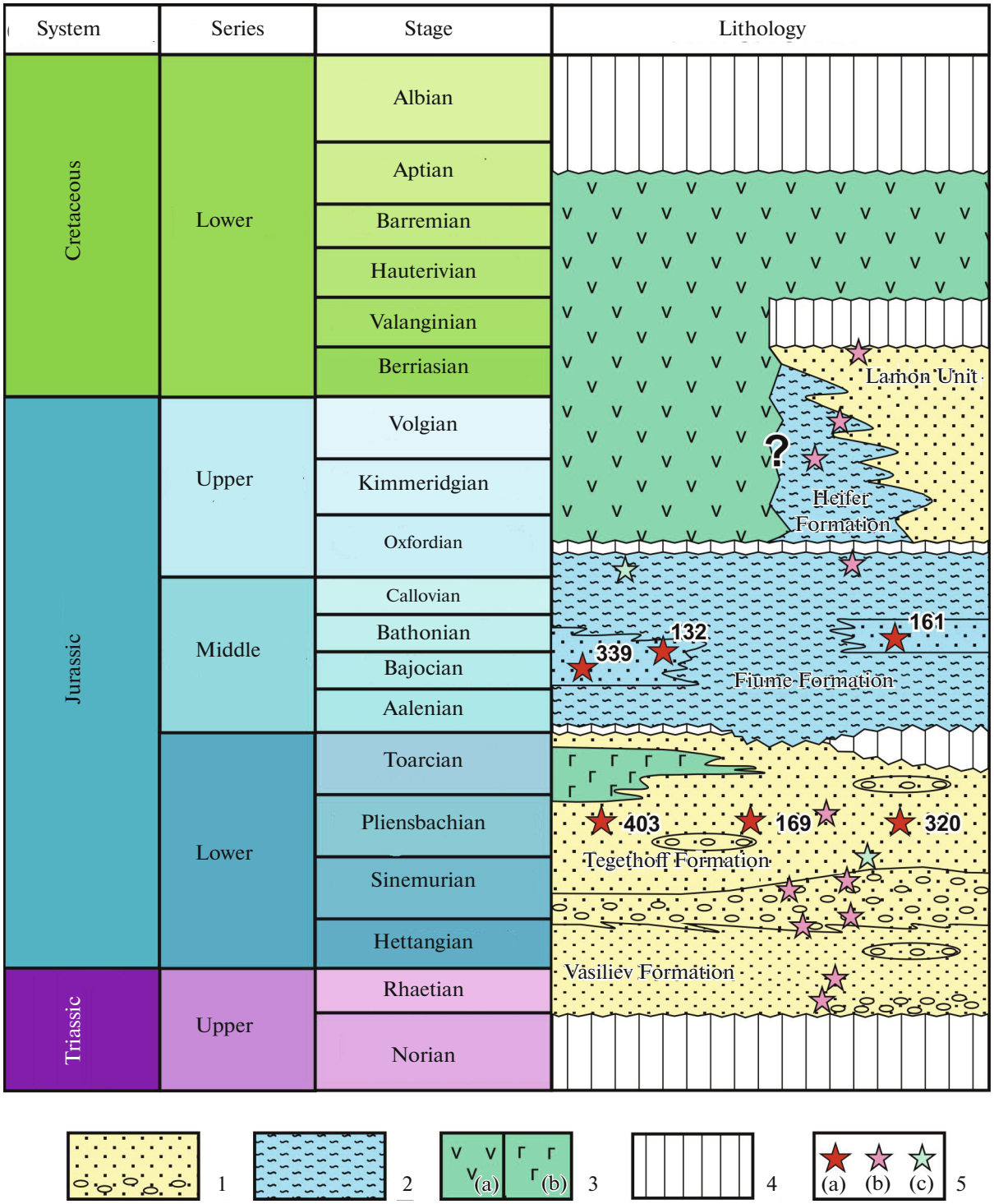

Fig. 2. Lithological-stratigraphic column of the Franz Josef Land (FJL) Archipelago. (1) Continental sands, sandstones, siltstones, gravelstones, conglomerates; (2) marine clays, siltstones, sands; (3) basalts, tuffs, tuff breccias, tuff conglomerates: (a) Late Jurassic–Early Cretaceous; (b) Early Jurassic; (4) hiatus; (5) detrital zircons samples: (a) outcrops described in this paper (with numbers), (b) outcrops after (Ershova et al., 2022), (c) after (Khudoley et al., 2019).

jurensis, *Verrucosisporites* sp., *Lophotriletes* cf. *bauchiniae*, *Granulatisporites* sp., *Foveosprorites* sp., *Cadargasporites* sp., *Pilasporites marcidus*, *Lycopodiumsporites* sp., etc. According to G.N. Aleksandrova, the pollen of gymnosperms is represented by *Inaperturpollenites* spp., *Alisporites* sp., *Piceapollenites* spp., *Pinuspollenites* sp., *Cicadopites orbicularis*, *C. percarinatus*, single *Exesipollenites tumulus*, *Quadraeculina annelae-*

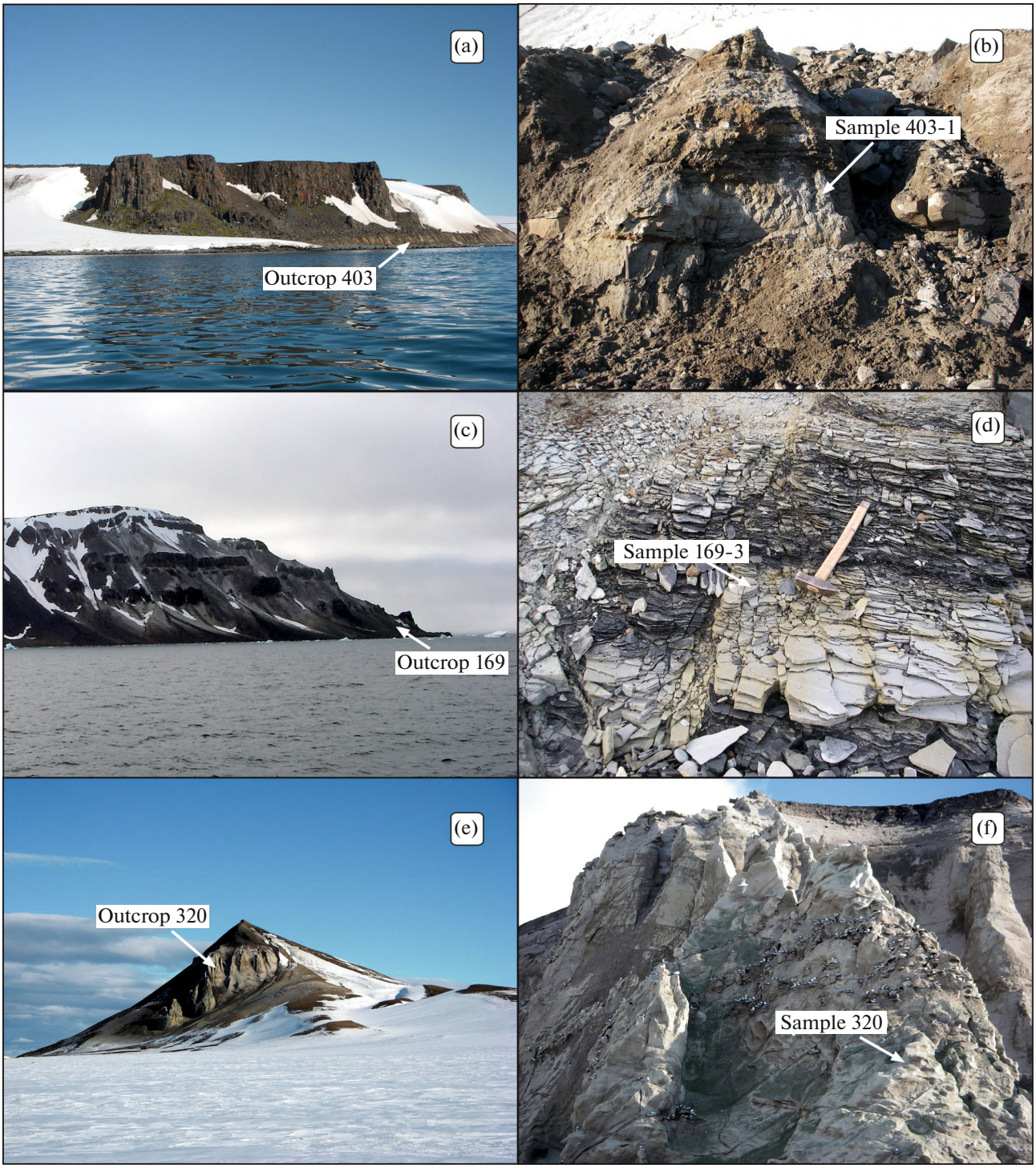

Fig. 3. Outcrops and sampling sites of Early Jurassic sedimentary rocks in the Franz Josef Land (FJL) Archipelago. (a, b) Hooker Island, Lunacharsky Rock; (c, d) Ziegler Island, Cape Brice; (e, f) Graham Bell Island, Mount Kohlsaat. Photo by Yu.V. Karyakin.

formis, and *Chasmatosporites hians*. The palynocomplexes similar in the composition were identified in Bajocian deposits of Northern Siberia (Ilyina, 1985).

On the southeastern coast of Hayes Island, at the elevation of 125 m (80°32′24.5″ N, 57°53′31.9″ E), a unit of gray, fine-, medium-, and coarse-grained subarkose was sampled, sometimes alternating with dark gray to black siltstones and mudstones (outcrop 132, Sample 132-3; Fig. 4c). The thickness of single sandstone beds ranges from the first tens of centimeters to 1.5–2 m, with an overall apparent thickness of 75–

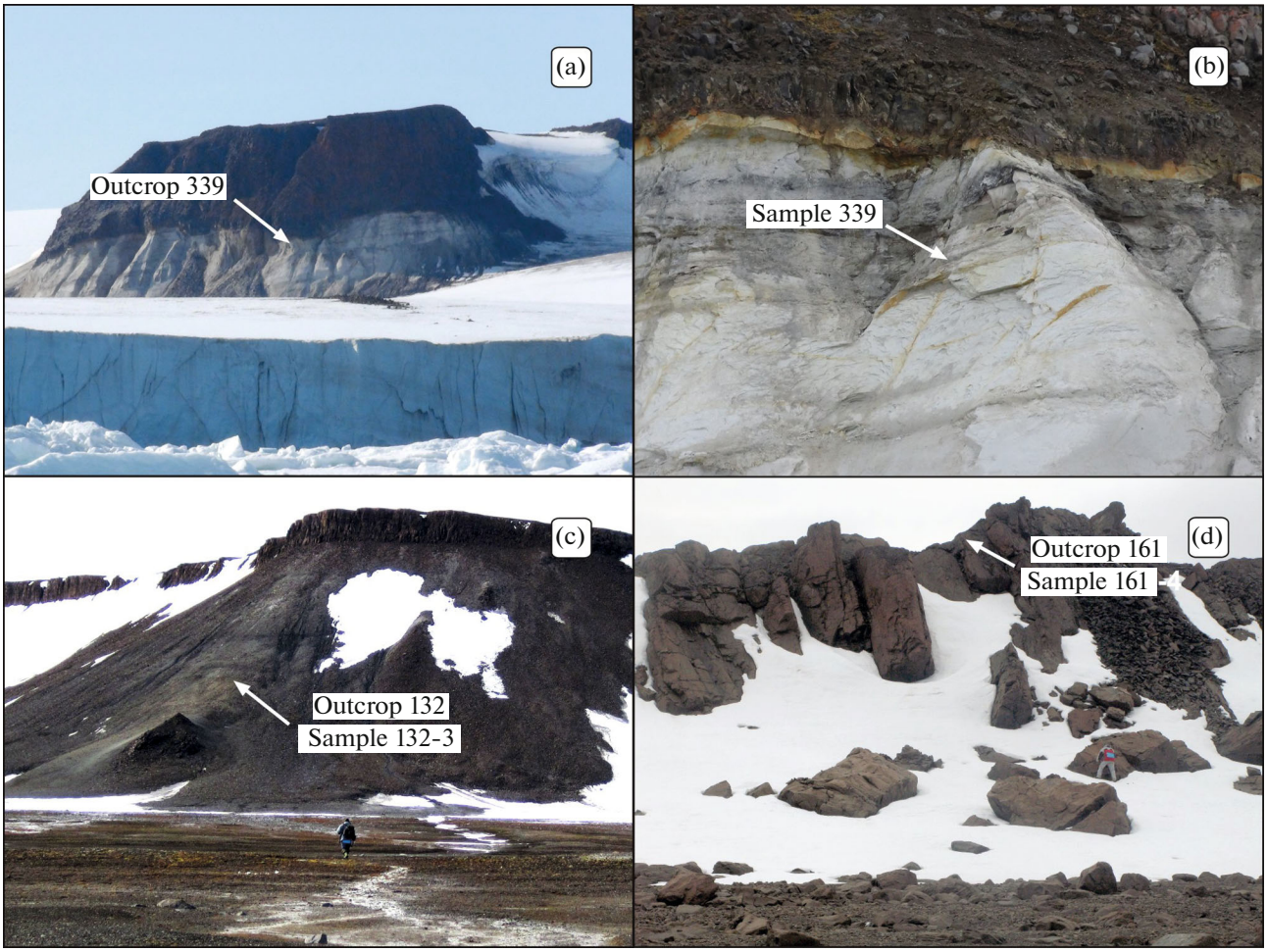

Fig. 4. Outcrops and sampling sites of Middle Jurassic sedimentary rocks in the Franz Josef Land (FJL) Archipelago. (a, b) Hooker Island, the outcrop 5 km to the northwest of Cape Al'banova; (c) Hayes Island, the 125 m elevation area, 6 km to the east-northeast of Cape Ostantsovy; (d) Jackson Island, Cape Kremsmunster. Image by Yu.V. Karyakin.

80 m. This unit extends along the strike of the entire southwestern coast of Hayes Island, with hiatuses, to the Krenkel meteorological station, where it is facially replaced by a black, thin-plated mudstones intruded by several basalt sills. Palynospectra similar to late Bajocian–Bathonian palynocomplexes were identified in mudstones and sandstones of this unit (Ilyina, 1985; *Unifitsirovannaya*..., 1993, 2012). This palynological assemblage is characterized by the predominance of gymnosperm spores over pollen, among which the following species are the most common: *Stereisporites* species (*S. bujargiensis*, *S. psilatus*, *S. incertus*, *S. congregatus*), *Cyathidites* spp., *Matonisporites* spp., *Lycopodiumsporites* spp. (including *L. intortivallus*), *Klukisporites variegatus*. According to T.F. Tregub, there is also *Lophotriletes torosus*.

At Cape Kremsmünster on Jackson Island (81°17′38.3″ N, 57°55′55.2″ E), a succession of gray, massive, fine-grained arkosic sandstones with an apparent thickness of 18–20 m was sampled. This unit overlies two flows of Early Cretaceous subalkaline basalts with no visible contact. In addition to quartz and feldspar, the sandstones contain (up to 25–30%) fragments of mesostasis of felsic volcanic rocks with devitrification structures, tuffaceous mudstones, detrital micas, and altered titanomagnetite. In these rocks (outcrop 161, Sample 161-4; Fig. 4d), a palynospectrum has been determined with frequent *Stereisporites bujargeiensis*, *S. congregatus*, *Sciadopityspollenites macroverrucosus*, *Lophotriletes torosus*, and *Klukisporites variegatus* and less common *Gleicheniidites*, *Sestrosporites pseudoalveolatus*, and *Marattisporites scabratus*. This palynocomplex corresponds to the regional palynocomplex with *Sestrosporites pseudoalveolatus* and *Sciadopityspollenites macroverrucosus* from the upper part of the Sysola Horizon–lower part of the Kurdyum Horizon (Ilyina, 1991; *Unifitsirovannye*..., 1993, 2012), which indicates the Bathonian age of the host rocks (conclusion by T.F. Tregub).

Thus, for U–Pb dating of detrital zircon grains from the Lower and Middle Jurassic sedimentary deposits of the FJL, we used six samples of sands and

Table 1. Operational parameters of equipment settings for U–Th–Pb (LA-ICP-MS) isotope dating of zircons

Equipment	Parameter	Value
Element 2 high-resolution (SF-ICP-MS) mass spectrometer	RF power generator	1200 W
	Argon, purity 99,998%:	
	cooling flow	16 L/min
	auxiliary flow	0.9–1.5 L/min
	sample-presentation flow	0.85–0.925 L/min
	Tube length from MS to LA	150 cm
	Cone material	Ni
	Resolution	Low
	Scan type	E-scan
	Detector dead time	20 ns
	Measurement method:	
	Measured masses	206, 207, 208, 232, 238
	Detection mode	Analogous/countable
	Mass scan window	4%
	Magnet delay time (ms)	12 (206), 16 (207), 8 (208; 232; 238)
	Measurement time (ms)	3 (206), 4 (207), 2 (208; 232; 238)
	Number of runs per pass	800
	Signal integration type	Arithmetic mean
	Number of signals at peak	100
Laser ablation system NWR-213 (LA)	Laser	Nd-YAG
	Ablation chamber	2Vol Cell
	Positioning accuracy	±1.5 μm
	Wave length	213 nm
	Pulse frequency	5–10 Hz
	Beam diameter	25 μm
	Energy density	5–10 J/cm^2
	Ablation time	25 s
	Helium, purity 99,9995%:	
	sample-presentation flow	0.9 L/min
	Background measurement time	15 s
	Average purge time	60 s
	Measurement mode	Ablation at point
	Setting	Linear scanning, 5 μm/s

sandstones from five islands in different parts of the archipelago. These samples were collected during fieldwork over many years (Fig. 1). The dates obtained allow us to reconstruct the evolution of the provenance areas during the Pliensbachian and Bajocian–Bathonian.

RESEARCH METHODOLOGY

Detrital zircons were extracted using a standard technique at the Laboratory of Fission-Track and Mineral Analysis at the Geological Institute of the Russian Academy of Sciences (GIN RAS, Moscow). The zircon grains were mounted in epoxy resin and polished until they were approximately half their original thickness. Cathodoluminescence images (CL images) of detrital zircons were taken at the Laboratory for Investigation of Rock-Forming Minerals by Physical Methods at GIN RAS using a TESCAN VEGA scanning electron microscope equipped with a CL detector.

The U–Pb (LA-ICP-MS) isotope dating of zircons from rocks was conducted at the Laboratory of

Table 2. Weighted average age values of the 91500 and Plesovice zircon standards obtained during five measurement sessions

Sample no.	91500		Plesoviče	
	n	Age $^{206}Pb/^{238}U$ Ma, ±2σ	*n*	Age $^{206}Pb/^{238}U$ Ma, ±2σ
403-1	14	1066.9 ± 6.0	14	337.0 ± 2.0
132-3	8	1066.5 ± 7.8	8	335.5 ± 2.7
320	7	1062.6 ± 7.8	9	336.8 ± 2.2
169-3	9	1068.4 ± 7.1	9	339.9 ± 2.4
161-4	9	1064.5 ± 7.1	9	334.8 ± 4.6
339	11	1061.1 ± 6.4	11	338.1 ± 4.6

n—number of measurements.

Analytical Chemistry at GIN RAS using an NWR-213 nanosecond laser ablation system (Electro Scientific Ind.), combined with an Element2 high-resolution sector field ICP mass spectrometer (Thermo Scientific Inc.). The operating parameters are given in Table 1. The technique of dating is described in (Sheshukov et al., 2018).

Calibration was performed using an external zircon GJ-1 standard (Jackson et al., 2004; Horstwood et al., 2016). To assess the quality of the analysis during the measurement of unknown zircon grains, control zircon 91500 (Wiedenbeck et al., 1995) and Plešovice (Sláma et al., 2008) standards were measured (Table 2). The weighted average $^{207}Pb/^{206}Pb$ and $^{206}Pb/^{238}U$ ages of zircon 91500 determined during the measurement of unknown zircons were 1064 ± 3 Ma (2σ, MSWD = 0.24, probability = 1.0, *n* = 57) and 1065 ± 3 Ma (2σ, MSWD = 0.34, probability = 1.0, *n* = 57), respectively, which is consistent with CA-ID-TIMS data (Horstwood et al., 2016). The weighted average $^{206}Pb/^{238}U$ age of the Plesoviče zircon was 337 ± 1 Ma (2σ, MSWD = 1.2, probability = 0.12, *n* = 52), which is consistent with the published CA-ID-TIMS data (Horstwood et al., 2016).

The isotope analysis data were processed and corrected using the Glitter software program (Van Achterbergh et al., 2001). Correction for common Pb was processed following the method developed by Andersen (2002) with use of the ComPbCorr software program (Andersen, 2008).

When constructing histograms and probability density curves, only zircon age estimates for which the discordance (*D*) was not greater than ±10% were taken into account. For zircon grains younger than 1000 Ma, the age was calculated on the basis of the $^{206}Pb/^{238}U$ isotope ratio; for older grains, it was based on $^{206}Pb/^{207}Pb$. Histograms and probability density curves of detrital zircon ages were constructed using the detzrcr software program (Andersen et al., 2018). The cumulative probability diagram of detrital zircon ages was constructed in a macro in MS EXCEL (Gehrels, 2006).

RESULTS OF RESEARCH

Sample 403-1, Hooker Island, Lunacharsky Rock (Tegethoff Formation, Pliensbachian). Zircon grains are semitransparent, yellow to pale yellow (60–65%), colorless (5–10%), and dark brown (30–35%) short prismatic and ellipsoidal. Slightly rounded and well-rounded grains with an elongation coefficient (EC) of 1–3 predominate (90%). The internal structure of the zircon grains in the CL image is simple, with oscillatory and less frequently sectoral zoning (Fig. 5a). Occasionally, there are grains with a homogeneous core surrounded by a rim with oscillatory zoning.

The U–Pb isotope system in 135 zircon grains was analyzed, and the results obtained from 131 analyses meet the selected discordance criterion (ESM). The age estimates obtained range from 2930 to 246 Ma (Fig. 6a). There are single zircon grains of Archean age, which do not form significant peaks on the relative probability density curve of zircon age distribution. In total, 18% of zircon grains yielded Paleoproterozoic ages and formed distinct peaks at ~1780 and 1670 Ma. Mesoproterozoic ages were obtained for 15% of zircon grains studied, with two age peaks of ~1180 and ~1100 Ma. Zircons with Neoproterozoic U–Pb ages account for 6% of the sample studied, with an age peak of ~640 Ma (Fig. 6b). Paleozoic dates are characteristic of 60% of the studied zircons. Among them, two main groups can be identified: Early Paleozoic, with peaks of 482, 442, and 410 Ma, and Late Devonian–Permian, with peaks of 385, 360, 342, and 310 Ma (Fig. 7f).

Sample 169-3, Ziegler Island, Cape Brice (Tegethoff Formation, Pliensbachian). Zircons are represented by transparent, colorless, pale yellow to pale pink (85%) crystals, less frequently by pale pink rounded grains (15%). Ellipsoidal and short prismatic well-rounded zircon grains with EC of 2–3 and their fragments (~70–80%) predominate. There are single weakly rounded crystals with EC > 3. As seen in the CL image, most grains have an oscillatory, less frequently homogeneous internal structure (Fig. 5b).

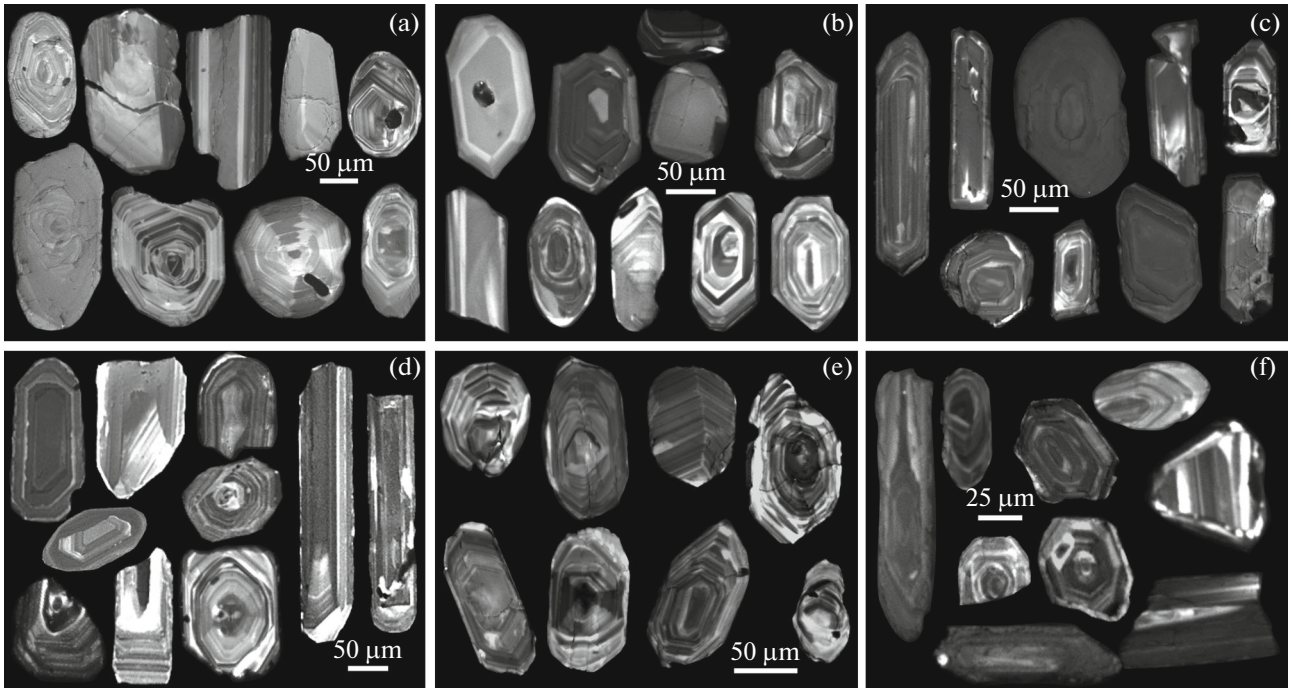

Fig. 5. CL images of detrital zircons from Early–Middle Jurassic sedimentary rocks of the Franz Josef Land (FJL) Archipelago. (a) Sample 403-1; (b) Sample 169-3; (c) Sample 320; (d) Sample 339; (e) Sample 132-3; (f) Sample 161-4.

U–Pb ages of zircon (n = 81) range from 2725 to 237 Ma (Fig. 6a). The Archean and Paleoproterozoic dates account for 21% of the total population and do not form significant age peaks on the probability density curve. Approximately 65% of zircon grains from the sample date to the Paleozoic. The Early–Middle Paleozoic ages yield peaks of 505, 455, 430, 410, and 368 Ma, while the Late Paleozoic ages yield peaks of 332, 300, and 282 Ma. The Triassic U–Pb age was obtained for 14% grains with an age peak of approximately 240 Ma (Fig. 7e).

Sample 320, Graham Bell Island, Cape Kohlsaat, Mount Kohlsaat (Tegethoff Formation, Pliensbachian). Zircons are represented by semitransparent, colorless, pale yellow to pale pink short-prismatic and, less frequently, long-prismatic grains with EC of 2 and 3, respectively. The weakly rounded crystals (65%) and isometric grains (20%) predominate. The rounded crystal fragments account for approximately 15% of the total number of zircon grains studied. The grains have a simple internal structure with oscillatory zoning; less frequently they are homogeneous (Fig. 5c).

U–Pb zircon ages (n = 80) range from 213 to 2635 Ma (Fig. 6a). Overall, 23% of zircon grains yielded the Precambrian ages without forming significant populations. Archean and Mesoproterozoic zircons are rare and account for only 7% of the entire sample studied. Among Mesoproterozoic zircons, those with an age of 1000–1200 Ma predominate, while among Neoproterozoic grains, those with an age of 560–820 Ma predominate (Fig. 6b). Paleozoic zircons (~72–73%) predominate. Among them, Early Paleozoic grains (30%) yield distinct age peaks at 458 and 433 Ma (Late Ordovician–Early Silurian); Late Paleozoic zircons (32–33%) have a small maximum at 365 Ma and well-defined peaks at about 335, 310, and 278 Ma (Fig. 7d). There are single Triassic grains (250–213 Ma).

Sample 339, Hooker Island, the outcrop 5 km northwest of Cape Al'banova (Fiume Formation, Bajocian). Zircons are represented by semitransparent, pale pink to pale yellow crystals, short prismatic and ellipsoidal in shape with EC of 1.5–2.5. Long prismatic zircon grains with EC of ~3 are less common. As seen in CL image, the zircon grains are homogeneous in their internal structure and characterized by oscillatory zoning, while grains with sectoral zoning or homogeneous are less common (Fig. 5d).

The U–Pb zircon ages obtained (n = 112) range from 202 to 3040 Ma (Fig. 6a). Approximately 23% of the zircon grains in the sample studied are Precambrian in age and do not form significant peaks on the relative probability curve. Most of the zircons (68%) are Paleozoic in age. Of these, 30% are Early Paleozoic with peaks at 445 and 418 Ma, and 28% are Late Paleozoic with age peaks at 355, 323, and 280 Ma. About 10% of the grains are Triassic in age, with an age peak of about 250 Ma (Fig. 7c).

Sample 132-3, the southeastern coast of Hayes Island, elevation of 125 m (Fiume Formation, late Bajocian–Bathonian). Zircons are represented by transparent, pale yellow to pale pink semitransparent grains of ellipsoidal and short prismatic shape, with EC of 1.5–2. About 55–60% of grains are weakly

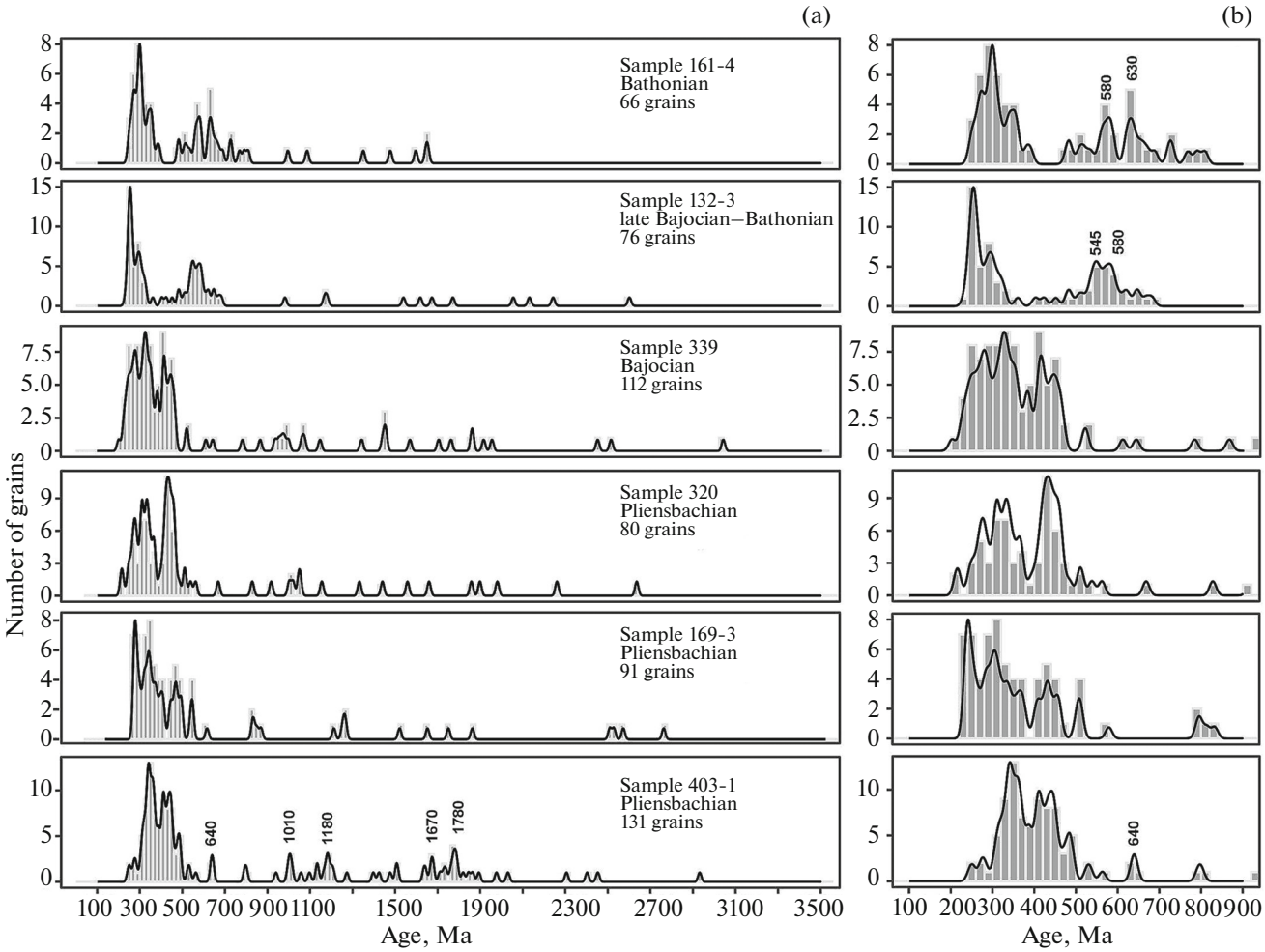

Fig. 6. Histograms and probability density curves of detrital zircon ages from Early–Middle Jurassic sandstones of the Franz Josef Land (FJL) Archipelago. (a) 100–3500 Ma; (b) 100–900 Ma. The age is determined for peaks based on at least three zircon grains in an age range older than 550 Ma.

slightly rounded. Well-rounded zircon grains account for 25% of the sample. Most grains have a homogeneous internal structure with oscillatory zoning. In some grains, this zoning has been violated (Fig. 5e).

The U–Pb zircon ages obtained (n = 76) range from 233 to 2600 Ma (Fig. 6a). Precambrian age values In total, 42% of the zircons have a Precambrian age, with groups with age peaks of 580 and 630 Ma (Fig. 6b). At this, 47% of the zircons yield the Paleozoic–Early Mesozoic dates, with two age peaks of 295 and 255 Ma (Early and Late Permian), and the predominant Early Triassic peak of about 250 Ma (Fig. 7b).

Sample 161-4, Jackson Island, Cape Kremsmunster (Fiume Formation, Bathonian). Zircons are represented by colorless and pale yellow semitransparent rounded grains of short prismatic shape (65%) with EC of 2–3. Weakly rounded crystals (10–15%) and sharp-angled fragments (15–20%) are less common. As seen in the CL image, most of the grains have a simple internal structure with oscillatory zoning (Fig. 5f).

The U–Pb ages of zircon (n = 66) range from 247 to 1654 Ma (Fig. 6a). Precambrian dates were obtained for 40% of the studied zircon grains, with two peaks at 580 and 630 Ma on the relative probability curve (Fig. 6b). Of these, 58% of the zircon grains yielded Paleozoic dates, with the most significant peak of 298 Ma. The age peaks of 275 and 345 Ma are less pronounced. An Early Triassic age of 247 ± 3 Ma was only obtained for one zircon grain.

DISCUSSION

The results of U–Pb dating of detrital zircons from Lower–Middle Jurassic sedimentary deposits of the FJL showed that the studied samples can be divided into two groups on the basis of the distribution of detrital zircon ages.

The first group (Fig. 8) combines samples from the Pliensbachian and Bajocian deposits (Samples 403-1, 169-3, 320, and 339). The Paleoproterozoic (approxi-

mately 1800–1600 Ma) and Mesoproterozoic (1300–1000 Ma) ages of detrital zircons from these samples can be correlated with magmatic and metamorphic events recorded in the terranes of the Baltica basement and Sveconorwegian–Grenville Orogen (for example, Andersson et al., 2004; Gorbatschev, 2004; Korja et al., 2006; Bogdanova et al., 2008). Similar in age, Mesoproterozoic complexes of the FJL basement were penetrated by the Nagursky borehole on Alexandra Land (Knudsen et al., 2019).

Neoproterozoic and Cambrian zircon dates (650–520 Ma) can be correlated with major magmatic and metamorphic events manifested within the Timanide Orogen (for example, Gee and Pease, 2004; Kuznetsov et al., 2007 and references therein). Moreover, zircons with Late Neoproterozoic–Early Cambrian (Timanides) ages are numerous in the Cambrian–Devonian deposits of the Kara Terrane, the Novaya Zemlya Archipelago, and the northeastern Baltica (e.g., Lorenz et al., 2008, 2013; Ershova et al., 2015, 2017b, 2019a, 2019b). On the basis of U–Pb dating of granite pebbles from Lower Jurassic conglomerates of Graham Bell Island, Ershova et al. (2022) proposed the occurrence of Timanide-aged magmatic rocks in the FJL archipelago.

Zircons with Early Paleozoic crystallization ages (480–410 Ma) may correspond to a coeval magmatic event, manifested only on the Severnaya Zemlya archipelago (Lorenz et al., 2007; Prokopiev et al., 2019; Kurapov et al., 2020). Moreover, Early Paleozoic detrital zircons are common in Paleozoic terrigenous rocks of the Svalbard (Beranek et al., 2020; Anfinson et al., 2022), Severnaya Zemlya (Lorenz et al., 2008; Ershova et al., 2015, 2018, 2019b), and Novaya Zemlya (Lorenz et al., 2013) archipelagos.

Detrital zircons with Late Paleozoic and Early Mesozoic crystallization ages, which are the most numerous among the dated grains, forms two distinct groups: Carboniferous–Early Permian (360–280 Ma) and Late Permian–Early Triassic (255–240 Ma). Late Paleozoic magmatic and tectonic events, associated with the closure of the Paleo-Ural Ocean, were widely manifested in the Arctic region (Şengör et al., 1993; Puchkov, 2009; Scott et al., 2010; Vernikovsky et al., 2013; Kurapov et al., 2021a). On the basis of U–Pb dating of zircons from pebbles of igneous rocks collected from Lower Jurassic conglomerates in the FJL area (Ershova et al., 2017a), it was suggested that Late Devonian–Carboniferous magmatism occurred in the northeast of the Barents Sea region. In addition, Late Paleozoic zircons are abundant in Triassic deposits of the Barents Sea region (Soloviev et al., 2015, 2023;

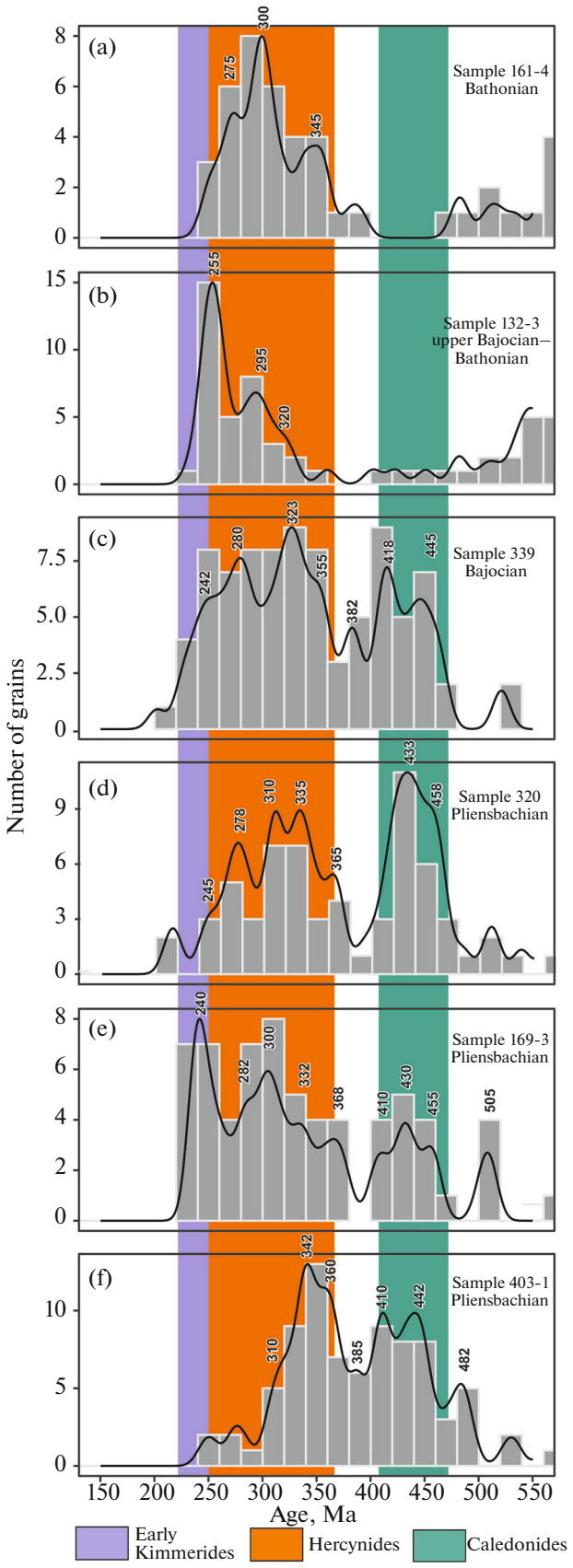

Fig. 7. Histograms and probability density curves of detrital zircon ages from Early–Middle Jurassic sands and sandstones (150–550 Ma) of the Franz Josef Land (FJL) Archipelago. The age is determined for peaks based on at least three zircon grains.

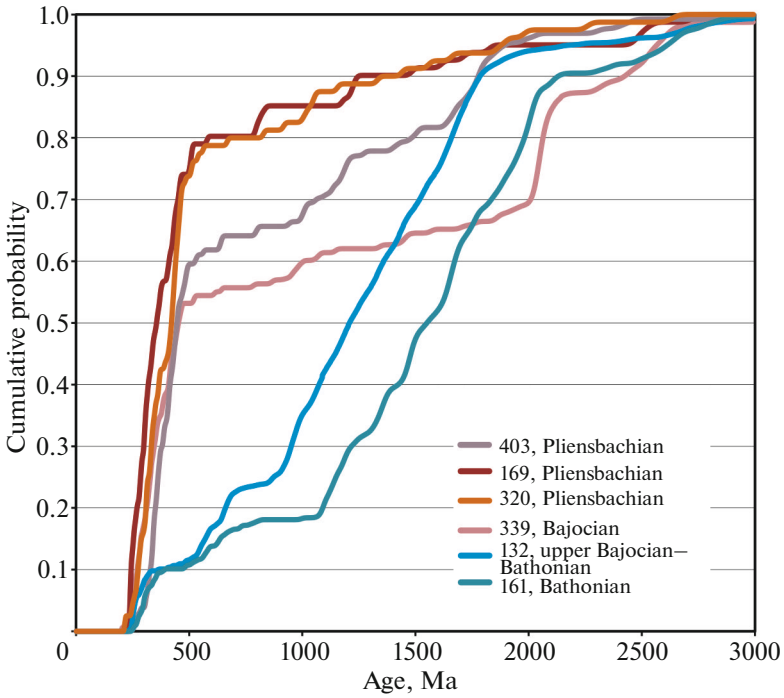

Fig. 8. Diagram of cumulative age probability of detrital zircon grains from Early–Middle Jurassic sands and sandstones of the Franz Josef Land (FJL) Archipelago.

Fleming et al., 2016; Klausen et al., 2017; Khudoley et al., 2018; Ershova et al., 2022).

The Late Permian–Triassic magmatism was manifested on the Taimyr Peninsula at approximately 255–225 Ma (Vernikovsky et al., 2003, 2020; Kurapov et al., 2021b). The Middle–Late Triassic detrital zircons are abundant in deposits that were penetrated by wells in the eastern and southwestern parts of the Barents Sea region (Fleming et al., 2016; Khudoley et al., 2018). Zircon grains with Triassic crystallization ages have been identified in Upper Triassic deposits of the Svalbard and Franz Josef Land archipelagos (Røhr and Andersen, 2009; Pózer Bue and Andresen, 2014).

The Lower Jurassic deposits in the FJL area are composed of coarse-grained feldspar-quartz sandstones, enclosing lenses and interbeds of gravelstone with well-rounded massive quartz and chalcedony pebbles. There are also thick units of polymictic conglomerates (Dibner, 1998; Ershova et al., 2022).

This indicates the close proximity of the provenance area to the sedimentation basin. Moreover, according to low-temperature thermochronology data, the provenance area supplying Lower Jurassic terrigenous deposits underwent significant uplift (up to 6 km) in the Late Triassic (Ershova et al., 2022).

The Late Triassic–Early Jurassic uplift is generally characteristic of the northeastern part of the Barents Sea basin, Taimyr, and possibly the North Kara basin (Zhang et al., 2018; Drachev and Ershova, 2024). The uplifts, composed of different-age metamorphic (Meso-Neoproterozoic), igneous (Cambrian and Late Devonian–Carboniferous), and Cambrian–Triassic metasedimentary and sedimentary rocks, were likely the main sources of clastic material.

The second group (Fig. 8) includes Samples 132-3 and 161-4, collected from Bathonian deposits in the FJL area. There are two main populations of detrital zircons—Late Proterozoic and Late Paleozoic (Figs. 7a, 7b). It should be noted that, in these samples, unlike earlier deposits, Early Paleozoic zircons are rare and do not form significant peaks on the relative probability curves of zircon age distribution. Our analysis of the potential provenance areas has revealed that the Permian deposits in the northern part of the Novaya Zemlya archipelago (Lorenz et al., 2013), Lower-Middle Triassic deposits in FJL (Soloviev et al., 2015), and Lower–Middle Triassic deposits in the eastern part of Barents Sea (Khudoley et al., 2018) have the most similar distribution of detrital zircon ages compared to those obtained for the Bathonian

Fig. 9. Histograms and probability density curves of detrital zircon ages from Triassic–Jurassic deposits of the Barents Sea region (Røhr and Andersen, 2009; Røhr et al., 2010; Pózer and Andresen, 2014; Soloviev et al., 2015; Fleming et al., 2016; Klausen et al., 2017; Khudoley et al., 2019; Ershova et al., 2022; this work;) and Permian deposits in the northern part of the Novaya Zemlya Archipelago (Lorenz et al., 2013). The diagrams marked with asterisks are characterized by the absence or insignificant amount of Early Paleozoic zircons.

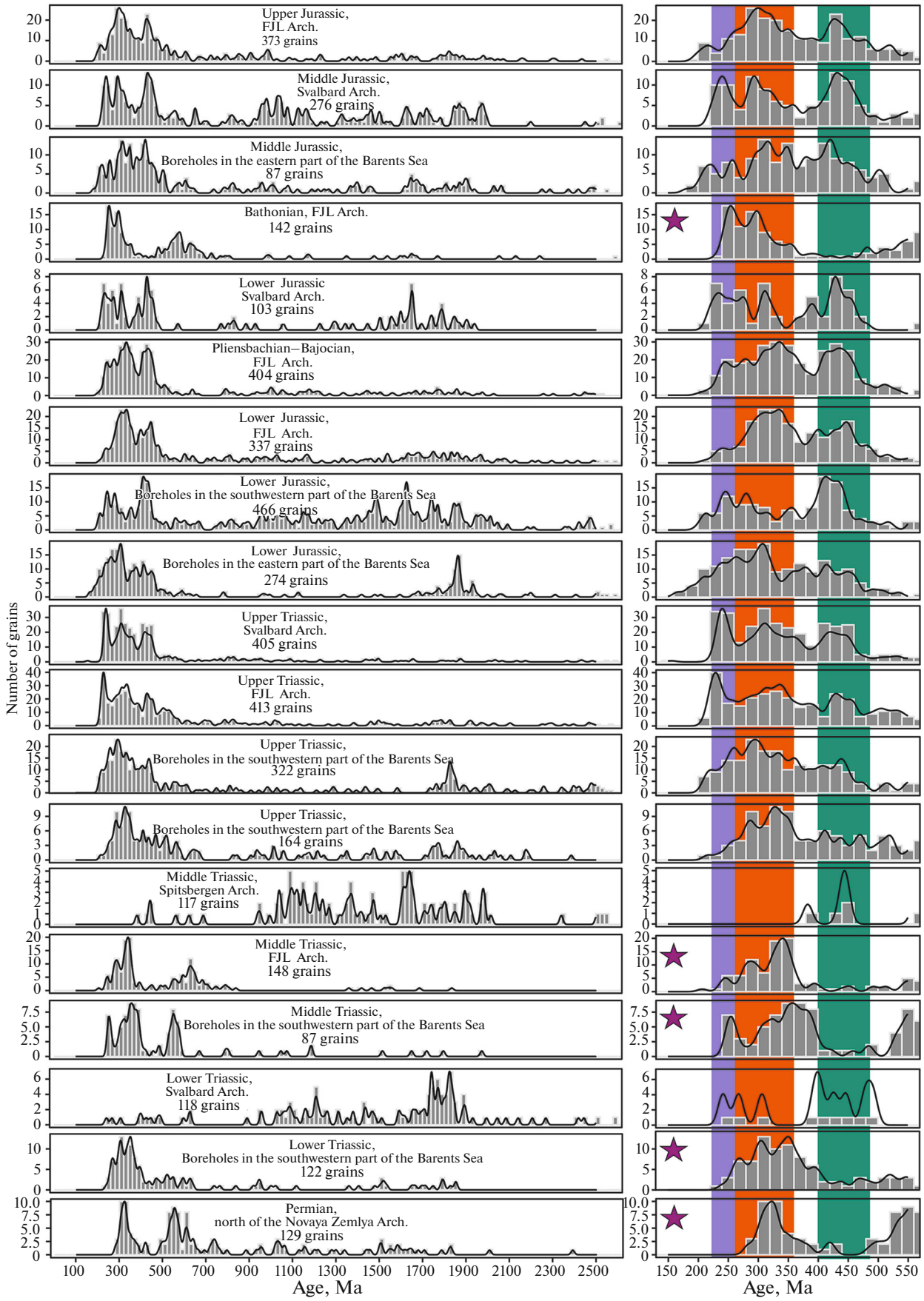
Upper Jurassic, FJL Arch. 373 grains
Middle Jurassic, Svalbard Arch. 276 grains
Middle Jurassic, Boreholes in the eastern part of the Barents Sea 87 grains
Bathonian, FJL Arch. 142 grains
Lower Jurassic Svalbard Arch. 103 grains
Pliensbachian–Bajocian, FJL Arch. 404 grains
Lower Jurassic, FJL Arch. 337 grains
Lower Jurassic, Boreholes in the southwestern part of the Barents Sea 466 grains
Lower Jurassic, Boreholes in the eastern part of the Barents Sea 274 grains
Upper Triassic, Svalbard Arch. 405 grains
Upper Triassic, FJL Arch. 413 grains
Upper Triassic, Boreholes in the southwestern part of the Barents Sea 322 grains
Upper Triassic, Boreholes in the southwestern part of the Barents Sea 164 grains
Middle Triassic, Spitsbergen Arch. 117 grains
Middle Triassic, FJL Arch. 148 grains
Middle Triassic, Boreholes in the southwestern part of the Barents Sea 87 grains
Lower Triassic, Svalbard Arch. 118 grains
Lower Triassic, Boreholes in the southwestern part of the Barents Sea 122 grains
Permian, north of the Novaya Zemlya Arch. 129 grains
Number of grains
100 300 500 700 900 1100 1300 1500 1700 1900 2100 2300 2500
Age, Ma
150 200 250 300 350 400 450 500 550
Age, Ma

deposits in the FJL area. The latter are characterized by the absence of Early Paleozoic zircons and the presence of zircons of two main age groups—Late Neoproterozoic and Late Paleozoic (Fig. 9). We suggest that the sources of detrital zircon grains underwent significant changes at the Bajocian–Bathonian boundary, as reflected in the U–Pb age distributions obtained in this study. It is likely that by the Middle Jurassic, most of the uplifts formed during the Late Triassic—which had served as major sources of clastic material throughout the Early Jurassic—had been extensively eroded. In addition, a major transgression beginning in the late Bajocian led to the expansion of marine sedimentation across the Barents Sea region (Smelror et al., 2001). These processes together resulted in a substantial reduction of continental land areas that could have supplied detrital input. The remaining source areas were likely limited to small regions composed of Permian and/or Lower to Middle Triassic deposits, which became the main sources of clastic grains for the Bathonian sediments of Franz Josef Land.

The evidence of erosion is supported by the presence of redeposited Triassic spores and pollen found in the sands of the Tegethoff Formation on Hooker Island (Karyakin and Aleksandrova, 2023). Intense local erosion of both Triassic and Early Jurassic deposits in the Middle–Late Jurassic is confirmed by the abundance of clinopyroxenes and black ore minerals (up to 85–89%) in the heavy fraction of Aalenian clays of the Fiume Formation. The light fraction contains mainly plagioclases (Dibner et al., 1962), which could have originated only from Early Jurassic basalts (Fig. 2). The flows of these basalts was discovered on southern islands of the archipelago—Hooker, Scott Keltie, May, Newton, and Leigh-Smith islands (Karyakin and Aleksandrova, 2023). On Leigh-Smith Island, the basalt flows overlies early Toarcian sands and is overlain by late Toarcian ones. The first clinopyroxene grains appear in late Toarcian sands, while they are absent in underlying early Toarcian sands. During the Kimmeridgian, the intensity of erosion decreased. The heavy fraction of Kimmeridgian deposits contains no more than 10–25% clinopyroxenes (Kosteva, 2002).

It is noteworthy that in the Oxfordian–Early Cretaceous deposits of Franz Josef Land, the detrital zircon age distributions once again resemble those obtained in this study, as well as those previously reported for the Early Jurassic strata of the archipelago (Ershova et al., 2022; Fig. 9). This likely reflects a renewed reorganization of the sedimentary basin and the re-exposure of source regions characteristic of the Early Jurassic, and/or the erosion of Late Triassic to Early Jurassic deposits during the Oxfordian to Early Cretaceous interval. This interpretation is consistent with a major regression documented at the Oxfordian boundary in the Barents Sea region, particularly in its better-studied Norwegian sector (Smelror et al., 2001). A significant hiatus in sedimentation during the Middle Oxfordian is also inferred for Franz Josef Land based on the work of N.N. Kosteva (Kosteva, 2002, 2005). It was likely this event that caused a shift in sediment provenance, an expansion of continental land areas in the Late Jurassic, and the exposure and erosion of source regions different in composition from those active during the Bathonian.

CONCLUSIONS

U–Pb dating of detrital zircons from Lower and Middle Jurassic deposits in the FJL has allowed us to characterize stratigraphic intervals that were not previously studied. Data for the northern and central parts of the archipelago have been obtained for the first time.

On the basis of the distribution of detrital zircon ages, the samples are divided into two groups.

The first group includes samples 403-1, 169-3, 320, and 339, which represent predominantly coarse-grained sandstones and gravelites of Pliensbachian and Bajocian age. These rocks contain thick beds of polymictic conglomerates, indicating a proximal position of the sediment source relative to the depositional basin. We suggest that the main sources of detritus were uplifts composed of metamorphic rocks of various ages (Meso- to Neoproterozoic), magmatic rocks (Cambrian and Late Devonian–Carboniferous), as well as Cambrian to Triassic sedimentary deposits.

The second group of samples includes those collected from the Bathonian deposits in the FJL area (132-3 and 161-4). These samples contain two main populations of detrital zircon—Late Neoproterozoic and Late Paleozoic. The Permian deposits in the northern part of the Novaya Zemlya Archipelago, Lower–Middle Triassic deposits in the FJL, and Lower–Middle Triassic deposits in the northeastern part of the Barents Sea region show the most similar distribution of detrital zircons ages compared to those obtained by us for the Bathonian deposits in the FJL. It is likely that during the Bathonian, the detrital material was delivered to the sedimentary basin through the recycling of Permian and/or Lower to Middle Triassic deposits of the Barents Sea region.

The studies conducted allow us to better understand the paleogeography of the FJL in the Jurassic. By the Middle Jurassic, most of the uplifted areas that became sources of detrital material for the Early Jurassic sedimentary basin had already been eroded, and an extensive transgression that began in the late Bajocian led to the expansion of the marine sedimentation in the Barents Sea region. This resulted in a significant reduction of the continental land area, and small areas of land composed of Permian and/or Lower–Middle Triassic deposits likely became the main provenance areas.

SUPPLEMENTARY INFORMATION

The online version contains supplementary material available at https://doi.org/10.1134/S0869593825700261.

ACKNOWLEDGMENTS

We would like to thank the staff of the Russian Arctic National Park for their assistance in organizing and conducting fieldwork in the Franz Josef Land Archipelago. We are grateful to T.F. Tregub (Voronezh State University) for the conclusions on the age of the palynocomplexes.

FUNDING

The research was conducted in accordance with the research plans of the Geological Institute, Russian Academy of Sciences, and was supported by the Russian Foundation for Basic Research, project no. 18-05-70040 led by S.Yu. Sokolov "Evolution of the Lithosphere of the Western Arctic: Processes, Mechanisms, Development Trends, Natural Resources, and Geological Hazards."

CONFLICT OF INTEREST

The authors of this work declare that they have no conflicts of interest.

Reviewers V.N. Kovach and A.B. Kotov

REFERENCES

Andersen, T., Correction of common lead in U–Pb analyses that do not report ^{204}Pb, *Chem. Geol.*, 2002, vol. 192, pp. 59–79.
https://doi.org/10.1016/S0009-2541(02)00195-X

Andersen, T., ComPbCorr—Software for common lead correction of U–Th–Pb analyses that do not report ^{204}Pb, in *LA-ICP-MS in the Earth Sciences: Principles and Applications*, Sylvester P.J., Ed., *Mineral. Assoc. Canada. Short Course Ser.*, 2008, vol. 40, pp. 312–314.

Andersen, T., Kristoffersen, M., and Elburg, M.A., Visualizing, interpreting and comparing detrital zircon age and Hf isotope data in basin analysis—a graphical approach, *Basin Res.*, 2018, vol. 30, pp. 132–147.
https://doi.org/10.1111/bre.12245

Andersson, U.B., Sjöström, H., Högdahl, K.H.O., and Eklund, O., The Transscandinavian Igneous Belt, evolutionary models, in The Transscandinavian Igneous Belt (TIB) in Sweden: A Review of its Character and Evolution, *Geol. Surv. Finland*, 2004, *Spec. Pap.* 37, pp. 104–112.

Anfinson, O.A., Odlum, M.L., Piepjohn, K., Poulaki, E.M., Shephard, G.E., Stockli, D.F., Levang, D., Jensen, M.A., and Pavlovskaia, E.A., Provenance analysis of the Andrée Land Basin and implications for the paleogeography of Svalbard in the Devonian, *Tectonics*, 2022, vol. 41, e2021TC007103.
https://doi.org/10.1029/2021TC007103

Barents shelf plate, in *Trudy VNIIOkeangeologiya. T. 196* (Trans. VNIIOkeangeologiya. Vol. 196), Gramberg, I.S., Ed., Leningrad: Nedra, 1988.

Basov, V.A., Pchelina, T.M., Vasilenko, L.V., Korchinskaya, M.V., and Fefilova L.A., Justification of age of the Mesozoic sedimentary sequences boundaries on the Barents Sea shelf, in *Stratigrafiya i paleontologiya Rossiiskoi Arktiki* (Stratigraphy and Paleontology of the Russian Arctic), St. Petersburg: VNIIOkeangeologiya, 1997, pp. 35–48.

Basov, V.A., Vasilenko, L.V., Viskunova, K.G., Korago, E.A., Korchinskaya, M.V., Kupriyanova, N. V., Povysheva, L.G., Preobrazhenskaya, E.N., Pchelina, T. M., Stolbov, N.M., Suvorova, E. B., Suprunenko, O.I., Suslova, V.V., Ustinov, N.V., Ustritskii, V.I., and Fefilova, L.A., Evolution of sedimentary environments in the Barents–North Kara Palaeobasin in the Phanerozoic, *Neftegaz. Geol. Teor. Prakt.*, 2009, no. 4, pp. 1–44.

Beranek, L.P., Gee, D.G., and Fisher, C.M., Detrital zircon U–Pb–Hf isotope signatures of Old Red Sandstone strata constrain the Silurian to Devonian paleogeography, tectonics, and crustal evolution of the Svalbard Caledonides, *GSA Bull.*, 2020, vol. 132, pp. 1987–2003.
https://doi.org/10.1130/B35318.1

Bogdanova, S. V., Bingen, B., Gorbatschev, R., Kheraskova, T.N., Kozlov, V.I., Puchkov, V.N., and Volozh, Yu.A., The East European Craton (Baltica) before and during the assembly of Rodinia, *Precambrian Res.*, 2008, vol. 160, nos. 1–2, pp. 23–45.
https://doi.org/10.1016/j.precamres.2007.04.024

Dibner, V.D., *Gosudarstvennaya geologicheskaya karta SSSR masshtaba 1 : 1000000, list VI-38, 39, 40, 41 (Zemlya Frantsa-Iosifa). Ob''yasnitel'naya zapiska* (The 1 : 1000000 State Geological Map of the USSR. Sheet VI-38, -39, -40, -41 (Franz-Josef Land). Explanatory Note), Moscow: Gosgeoltekhizdat, 1957.

Dibner, V.D., Islands in the Barents Sea, in *Geologiya SSSR. T. XXVI* (Geology of the USSR, Vol. XXVI), Moscow: Nedra, 1970, pp. 60–108.

Dibner, V.D. and Sedova, M.A., Materials on geology and biostratigraphy of the Upper Triassic and Lower Jurassic deposits of the Franz Josef Land, *Tr. NIIGA*, 1959, vol. 65, pp. 16–43.

Dibner, V.D., Razin, V.K., and Ronkina, Z.Z., The lithology and conditions for the formation of the Mesozoic deposits of the Franz Josef Land., *Tr. NIIGA*, 1962, vol. 121, pp. 44–74.

Drachev, S.S. and Ershova, V.B., North Kara and Vize–Ushakov composite tectono-sedimentary elements, Kara Sea, *Geol. Soc. London, Mem.*, 2024, vol. 57, no. 1.
https://doi.org/10.1144/M57-2023-13

Geology of Franz Josef Land, Dibner, V.D., Ed., Norsk Polarinst. Meddelelser, Oslo, 1998, vol. 146.

Ershova, V.B., Prokopiev, A.V., Khudoley, A.K., Shneider, G.V., Andersen, T., Kullerud, K., Makar'ev, A.A., Maslov, A.V., and Kolchanov, D.A., Results of U–Pb (LA–ICPMS) dating of detrital zircons from metaterrigenous rocks of the basement of the North Kara basin, *Dokl. Earth Sci.*, 2015, vol. 464, no. 4, pp. 997–1000.

Ershova, V.B., Prokopiev, A.V., Sobolev, N.N., Petrov, E.O., Khudoley, A.K., Faleida, Ya.I., Gaina, K., and Belyakova, R.V., New data on the basement of Franz Josef Land, Arctic region, *Geotectonics*, 2017a, no. 2, pp. 121–130.

Ershova, V.B., Prokopiev, A.V., Khudoley, A.K., Proskurnin, V.F., Andersen, T., Kullerud, K., Stepunina, M.A., and Kolchanov, D.A., New U–Pb isotopic data for detrital zircons from metasedimentary sequences of northwestern Taimyr, *Dokl. Earth Sci.*, 2017b, vol. 474, no. 2, pp. 613–616.

Ershova, V., Anfinson, O., Prokopiev, A., Khudoley, A., Stockli, D., Faleide, J.I., Gainae, C., and Malyshev, N., Detrital zircon (U–Th)/He ages from Paleozoic strata of

the Severnaya Zemlya Archipelago: deciphering multiple episodes of Paleozoic tectonic evolution within the Russian High Arctic, *J. Geodynam*., 2018, vol. 119, pp. 210–220. https://doi.org/10.1016/j.jog.2018.02.007

Ershova, V.B., Ivleva, A.S., Podkovyrov, V.N., Khudoley, A.K., Fedorov, P.V., Stockli, D., Anfindon, O., Maslov, A.V., and Khubanov, V., Detrital zircon (U–Th)/He ages from Paleozoic strata of the Severnaya Zemlya Archipelago: Deciphering multiple episodes of Paleozoic tectonic evolution within the Russian High Arctic, *GFF*, 2019a, vol. 141, no. 4, pp. 279–288. https://doi.org/10.1080/11035897.2019.1625073

Ershova, V.B., Prokopiev, A.V., Khudoley, A.K., Andersen, T., Kullerud, K., and Kolchanov, D.A., U–Pb age and Hf isotope geochemistry of detrital zircons from Cambrian sandstones of the Severnaya Zemlya Archipelago and Northern Taimyr (Russian High Arctic), *Minerals*, 2019b, vol. 10, no. 1. https://doi.org/10.3390/min10010036

Ershova, V., Prokopiev, A., Stockli, D., Kurapov, M., Kosteva, N., Rogov, M., Khudoley, A., and Petrov, E.O., Provenance of the Mesozoic Succession of Franz Josef Land (North-Eastern Barents Sea): paleogeographic and tectonic implications for the High Arctic, *Tectonics*, 2022, vol. 41. https://doi.org/10.1029/2022TC007348

Fleming, E.J., Flowerdew, M.J., Smyth, H.R., Scott, R.A., Morton, A.C., Omma, J.E., Frei, D., and Whitehouse, M.J., Provenance of Triassic sandstones on the southwest Barents Shelf and the implication for sediment dispersal patterns in northwest Pangaea, *Mar. Petrol. Geol.*, 2016, vol. 78, pp. 516–535. https://doi.org/10.1016/j.marpetgeo.2016.10.005

Gee, D.G. and Pease, V., The Neoproterozoic Timanide Orogen of eastern Baltica: Introduction, *Geol. Soc. London, Mem*., 2004, vol. 30, no. 1, pp. 1–3. https://doi.org/10.1144/gsl.mem.2004.030.01.01

Gehrels, G., *Analysis Tools*. http://www.geo.arizona.edu/alc/Analysis/Tools.htm

Gorbatschev, R., The Transscandinavian Igneous Belt – introduction and background, in *The Transscandinavian Igneous Belt (TIB) in Sweden: A Review of its Character and Evolution. Geol. Surv. Fin. Spec. Pap*., 2004, vol. 37, pp. 9–15.

Gramberg, I.S., Shkola, I.V., Bro, E.G., Shekhodanov, V.A. and Armishev, A.M., Parametric boreholes on islands of the Barents and Kara seas, *Sov. Geol.*, 1985, no. 1, pp. 95–98.

Grantz, A., Geophysical and geologic evidence that Amerasian basin, Arctic ocean, was created by two phases of anticlockwise rotation, in *Abstr. 102nd Annu. Meet. Cordillerran Sect. Sess. No. 42. AAPG/GSA: Geology of the Circum-Arctic, SPE (May 8–10, 2006). Pap. № 42-4. Geol. Soc. Am*., 2006, vol. 38, no. 5.

Grantz, A., Clark, D.L., Phillips, R.L., Srivastava, S.P., Blome, C.D., Gray, L.B., Haga, H., and Willard, D.A., Phanerozoic stratigraphy of Northwind Ridge, magnetic anomalies in the Canada basin, and the geometry and timing of rifting in the Amerasia basin, Arctic Ocean, *Geology*, 1998, vol. 110, no. 6, pp. 801–820. https://doi.org/10.1130/0016-7606(1998)110<0801:PSONRM>2.3.CO;2

Horstwood, M.S., Košler, J., Gehrels, G., Jackson, S.E., McLean, N.M., Paton, C., Pearson, N.J., Sircombe, K., Sylvester, P., Vermeesch, P., Bowring, J.F., Condon, D.J., and Schoene, B., Community-derived standards for LA-ICP-MS U–(Th–)Pb geochronology – Uncertainty propagation, age interpretation and data reporting, *Geostand. Geoanalyt. Res*., 2016, vol. 40, no. 3, pp. 311–332. https://doi.org/10.1111/j.1751-908X.2016.00379.x

Ilyina, V.I., Jurassic palynology of Siberia, in *Trudy IGiG SO AN SSSR* (Trans. Inst. Geol. Geophys. Sib. Br. USSR Acad. Sci.), Moscow: Nauka, 1985, vol. 638.

Ilyina, V.I., The dinocysts zonation of the Bathonian–Oxfordian deposits of the Russian Platform, in *Stratigrafiya i paleogeografiya osadochnykh tolshch neftegazonosnykh basseinov SSSR* (Stratigraphy and Paleogeography of Sedimentary strata in Oil-and-Gas Basins of the USSR), Leningrad: Vseross. Neft. Nauchno-Issled. Geol. Inst., 1991, pp. 42–64.

Jackson, S.E., Pearson, N.J., Griffin, W.L., and Belousova, E.A., The application of laser ablation-inductively coupled plasma-mass spectrometry to in situ U–Pb zircon geochronology, *Chem. Geol.*, 2004, vol. 211, pp. 47–69. https://doi.org/10.1016/J.CHEMGEO.2004.06.017

Karyakin, Yu.V. and Aleksandrova, G.N., Early Jurassic flood basalt volcanism on Franz Josef Land Archipelago: Geological and palynostratigraphical data, *Stratigr. Geol. Correl.*, 2023, vol. 31, no.1, pp. S23–S46. https://doi.org/10.31857/S0869592X23010039

Karyakin, Yu.V. and Sokolov, S.Yu., Assessment of the linear magnetic anomalies age at the territory of Franz-Joseph Land archipelago by geological data, in *Problemy tektoniki i geodinamiki zemnoi kory i mantii. Mater. L Tekton. soveshch.* (Problems of Tectonics and Geodynamics of the Earth's Crust and Mantle. Proc. L Tecton. Conf.), Moscow: GEOS, 2018, vol. 1, pp. 256–262.

Karyakin, Yu.V., Sklyarov, E.V., and Travin, A.V., Plume magmatism at Franz Josef Land, *Petrology*, 2021, vol. 29, no. 5, pp. 528–560. https://doi.org/10.1134/S0869591121050027

Khudoley, A.K., Verzhbitsky, V.E., Zastrozhnov, D.A., O'Sullivan, P., Ershova, V.B., Proskurnin, V.F., Tuchkova, M.I., Rogov, M.A., Kyserg, T.K., Sergey, V., Malyshev, S.V., and Schneider, G.V., Late Paleozoic–Mesozoic tectonic evolution of the Eastern Taimyr-Severnaya Zemlya Fold and Thrust Belt and adjoining Yenisey–Khatanga Depression, *J. Geodynam*., 2018, vol. 119, pp. 221–241. https://doi.org/10.1016/j.jog.2018.02.002

Khudoley, A.K., Sobolev, N.N., Petrov, E.O., Ershova, V.B., Makariev, A.A., Makarieva, E.V., Gaina, C., and Sobolev, P.O., A reconnaissance provenance study of Triassic–Jurassic clastic rocks of the Russian Barents Sea, *GFF*, 2019, vol. 141, no. 4, pp. 263–271. https://doi.org/10.1080/11035897.2019.1621372

Klausen, T.G., Müller, R., Slama, J., and Helland-Hansen, W., Evidence for Late Triassic provenance areas and Early Jurassic sediment supply turnover in the Barents Sea Basin of northern Pangea, *Lithosphere*, 2017, vol. 9, no. 1, pp. 14–28. https://doi.org/10.1130/L556.1

Knudsen, C., Gee, D.G., Sherlock, S.C., and Yu, L., Caledonian metamorphism of metasediments from Franz Josef Land, *GFF*, 2019, vol. 141, no. 4, pp. 295–307. https://doi.org/10.1080/11035897.2019.1622151

Korja, A., Lahtinen, R., and Nironen, M., The Svecofennian orogen: A collage of microcontinents and island arcs, *Geol. Soc. London, Mem*., 2006, vol. 32, no. 1, pp. 561–578. https://doi.org/10.1144/ gsl.mem.2006.032.01.34

Kosteva, N.N., Lithostratigraphy of the Mesozoic deposits on the Franz Josef Land Archipelago, *Cand. Sci. (Geol.-Mineral.) Dissertation*, St. Petersburg: St. Petersburg State Univ., 2002.

Kosteva, N.N., Stratigraphy of the Jurassic–Cretaceous deposits in the Franz Josef Land Archipelago, in *Arktika i Antarktika* (The Arctic and the Antarctic), Moscow: Nauka, 2005, vol. 4(38), pp. 16–32.

Kurapov, M., Ershova, V., Khudoley, A., Makariev, A., and Makarieva, E., The first evidence of Late Ordovician magmatism of the October Revolution Island (Severnaya Zemlya archipelago, Russian High Arctic): Geochronology, geochemistry, and geodynamic settings, *Norw. J. Geol.*, 2020, vol. 100, no. 1, pp. 1–15.
https://doi.org/10.17850/njg100-3-4

Kurapov, M., Ershova, V., Khudoley, A., Luchitskaya, M., Makariev, A., Makarieva, E., and Vishnevskaya, I., Late Palaeozoic magmatism of Northern Taimyr: new insights into the tectonic evolution of the Russian High Arctic, *Int. Geol. Rev.*, 2021a, vol. 63, no. 16, pp. 1–23.
https://doi.org/10.1080/00206814.2020.1818300

Kurapov, M., Ershova, V., Khudoley, A., Luchitskaya, M., Stockli, D., Makariev, A., Makarieva, E., and Vishnevskaya, I., Latest Permian–Triassic magmatism of the Taimyr Peninsula: New evidence for a connection to the Siberian Traps large igneous province, *Geosphere*, 2021b, vol. 17, no. 6, pp. 2062– 2077.
https://doi.org /10.1130/GES02421.1

Kuznetsov, N., Soboleva, A., Udoratina, O., Hertseva, M., and Andreichev, V., Pre-Ordovician tectonic evolution and volcano-plutonic associations of the Timanides and northern Pre-Uralides, northeast part of the East European Craton, *Gondwana Res.*, 2007, vol. 12, no. 3, pp. 305–323.
https://doi.org/10.1016/j.gr.2006.10.021

Lorenz, H., Gee, D.G., and Whitehouse, M.J., New geochronological data on Palaeozoic igneous activity and deformation in the Severnaya Zemlya Archipelago, Russia, and implications for the development of the Eurasian Arctic margin, *Geol. Mag.*, 2007, vol. 144, no. 1, pp. 105–125.
https://doi.org/10.1017/S001675680600272X

Lorenz, H., Gee, D.G., and Simonetti, A., Detrital zircon ages and provenance of the late Neoproterozoic and Palaeozoic successions on Severnaya Zemlya, Kara shelf: A tie to Baltica, *Norsk Geol. Tidsskrift*, 2008, vol. 88, no. 4, pp. 235–258.

Lorenz, H., Gee, D.G., Korago, E., Kovaleva, G., McClelland, W.C., Gilotti, J.A., and Frei, D., Detrital zircon geochronology of Palaeozoic Novaya Zemlya—A key to understanding the basement of the Barents Shelf, *Terra Nova*, 2013, vol. 25, no. 6, pp. 496–503.
https://doi.org/10.1111/ter.12064

Mickey, M.B., Byrnes, A.P., and Haga, H., Biostratigraphic evidence for the pre-rift position of the North Slope, Alaska, and Arctic Islands, Canada, and Sinemurian incipient rifting of the Canada Basin, in *Tectonic Evolution of the Bering Shelf–Chukchi Sea-Arctic Margin and Adjacent Landmasses: Boulder, Colorado*, Miller, E.L., Grantz, A., and Klemperer, S.L. Eds., *Spec. Paper—Geol. Soc. Am.*, 2002, vol. 360, pp. 67–75.

Pchelina, T.M., Paleogeographic reconstructions of the Barents–Kara region during the Triassic in relation to oil and gas potential, in *Trudy Tret'ei Mezhd. konf. "Osvoenie shel'fa Arkticheskikh morei Rossii"* (Proc. 3 Int. Conf. "The Development of the Shelf Zones of the Arctic Seas of Russia"), St. Petersburg: TsNII im. Akad. A.N. Krylova, 1998, pp. 261–263.

Pózer Bue, E. and Andresen, A., Constraining depositional models in the Barents Sea region using detrital zircon U–Pb data from Mesozoic sediments in Svalbard, *Spec. Publ.—Geol. Soc. London*, 2014, vol. 386, no. 1, pp. 261–279.
https://doi.org/10.1144/SP386.14

Preobrazhenskaya, E.N., Shkola, I.V., and Korchinskaya, M.V., Stratigraphy of Triassic deposits in the Franz Josef Land Archipelago (according to stratigraphic drilling data), in *Stratigrafiya i paleontologiya mezozoiskikh osadochnykh basseinov Severa SSSR* (Stratigraphy and Paleontology of the Mesozoic Sedimentary Basins in the North of the USSR), Leningrad: PGO "Sevmorgeologiya", 1985, pp. 5–15.

Prokopiev, A.V., Ershova, V.B., Sobolev, N.N., Korago, E., Petrov, E., and Khudoley, A.K., New data on geochemistry, age and geodynamic settings of felsic and mafic magmatism of the northeastern part of October Revolution Island (Severnaya Zemlya Archipelago), in *AGU Chapman Conf. "Large-Scale Volcanism in the Arctic: The Role of the Mantle and Tectonics,"* Selfoss, Iceland, 2019.

Puchkov, V.N., The evolution of the Uralian orogen, *Spec. Publ.—Geol. Soc. London*, 2009, vol. 327, no. 1, pp. 161–195.
https://doi.org/10.1144/SP327.9

Repin, Yu.S., Polubotko, I.V., Kiritchkova, A.I., and Kulikova, N.K., The sedimentary Mesozoic in the Franz Josef Land Archipelago (FJL), in *Voprosy stratigrafii, paleontologii i paleogeografii* (Problems of Stratigraphy, Paleontology, and Paleogeography), St. Petersburg: St. Petersburg State Univ., 2007, pp. 56–76.

Røhr, T. S. and Andersen, T., Detrital zircons from the high Arctic; evidence for extensive recycling of sediment from Devonian through Mesozoic times, in *Sedimentary Provenance Analysis of Lower Cretaceous Sedimentary Successions in The Arctic*; *Constraints From Detrital Zircon data*, *PhD Thesis*, Røhr, T. S., Ed., Faculty of Mathematics and Natural Sciences, Univ. Oslo, 2009, pp. 55–105.

Røhr, T.S., Andersen, T., Dypvik, H., and Embry, A.F., Detrital zircon characteristics of the Lower Cretaceous Isachsen Formation, Sverdrup Basin: Source constraints from age and Hf isotope data, *Can. J. Earth Sci.*, 2010, vol. 47, no. 3, pp. 255–271.
https://doi.org/10.1139/E10-006

Scott, R.A., Howard, J.P., Guo, L., Schekoldin, R., and Pease, V., Offset and curvature of the Novaya Zemlya fold-and-thrust belt, Arctic Russia, *Geol. Soc. London Petrol. Geol. Conf. Ser.*, 2010, vol. 7, no. 1, pp. 645–657.
https://doi.org/10.1144/0070645

Şengör, A.M.C., Natal'in, B., and Burtman, V.S., Evolution of the Altaid tectonic collage and Palaeozoic crustal growth in Eurasia, *Nature*, 1993, vol. 364, no. 6435, pp. 299–307.
https://doi.org/10.1038/364299a0

Sheshukov, V.S., Kuzmichev, A.B., Dubenskiy, A.S., Okina, O.I., Degtyarev, K.E., Kanygina, N.A., Kuznetsov, N.B., Romanjuk, T.V., and Lyapunov, S.M., U–Pb zircon dating by LA-SF-ICPMS at Geological Institute GIN RAS (Moscow), in *Abstr. 10th Int. Conf. of the Analysis of Geological and Environmental Materials*, Sydney, 2018.

Sláma, J., Košler, J., Condon, D.J., Crowley, J.L., Gerdes, A., Hanchar, J.M., Horstwood, M.S.A., Morris, G.A., Nasdala, L., Norberg, N., Schaltegger, U., Schoene, B.,

Tubrett, M.N., and Whitehouse, M.J., Plešovice zircon—A new natural reference material for U–Pb and Hf isotopic microanalysis, *Chem. Geol.*, 2008, vol. 249, pp. 1–35. https://doi.org/10.1016/J.CHEMGEO.2007.11.005

Smelror, M., Mørk, A., Mork, M.B.E., Weiss, H.M., and Løseth, H., Middle Jurassic–Lower Cretaceous transgressive-regressive sequences and facies distribution off northern Nordland and Troms, Norway. Sedimentary Environments Offshore Norway, *Proc. Norwegian Petrol. Soc. Conf. "Palaeozoic to Recent"*, 2001, pp. 211–232.

Soloviev, A.V., Zaionchek, A.V., Suprunenko, O.I., Brekke, H., Faleide, J.I., Rozhkova, D.V., Khisamutdinova, A.I., Stolbov, N.M., and Hourigan, J.K., Evolution of the provenances of Triassic rocks in Franz Josef Land: U/Pb LA-ICP-MS dating of the detrital zircon from well Severnaya, *Lithol. Miner. Resour.*, 2015, vol. 50, no. 2, pp. 102–116. https://doi.org/10.1134/S0024490215020054

Soloviev, A.V., Sobolev, P.O., Grushevskaya, O.V., Vasil'eva, E.A., Levochskaya, D.V., Khisamutdinova, A.I., Prokof'ev, I.N., Shimanskii, S.V., Belova, M.A., and Hourigan, J.K., Evolution of provenance areas and petroleum potential of Barents Sea Mesozoic deposits: dating of clastic zircon from Fersmanovskaya-1 well and paleogeography reconstructions, *Geol. Nefti Gaza*, 2023, no. 3, pp. 105–124. https://doi.org
https://doi.org/10.41748/0016-7894-2023-3-105-124

Stolbov, N.M., Kosteva, N.N., Basov, V.A., and Ustinov, N.V., The Stevens stratum: A new subdivision in the stratigraphy of the Franz Josef Land Archipelago, in *Geologo-geofizicheskie kharakteristiki litosfery Arkticheskogo regiona. Trudy NIIGA-VNIIOkeangeologiya* (Geological-Geophysical Features of the Lithosphere of the Arctic Region. Trans. NIIGA-VNIIOkeangeologiya), 2004, vol. 203, no. 5, pp. 232–234.

Stolbov, N.M., Basov, V.A., Suvorova, E.B., and Kosteva, N.N., New microfaunistic data on the Fiume Formation (J_{1-3}fm), Franz Josef Land Archipelago, in *Geologo-geofizicheskie kharakteristiki litosfery Arkticheskogo regiona. Tr. VNII-Okeangeologiya* (Geological-Geophysical Features of the Lithosphere of the Arctic Region. Trans. NIIGA-VNII-Okeangeologiya), 2010, vol. 210, no. 7, pp. 111–117.

Unifitsirovannaya regional'naya stratigraficheskaya skhema yurskikh otlozhenii Vostochno-Evropeiskoi platformy (14 listov). Ob"yasnitel'naya zapiska (Unified Regional Stratigraphic Scheme of Jurassic Deposits of the East European Platform (14 Sheets), Explanatory Note), Moscow: Paleontol. Inst. Ross. Akad. Nauk, VNIGNI, 2012.

Unifitsirovannaya stratigraficheskaya skhema yurskikh otlozhenii Russkoi platformy (Unified Regional Stratigraphic Scheme of Jurassic Deposits of the Russian Platform), St. Petersburg: Roskomnedra (VNIGRI), 1993.

Van Achterbergh, E., Ryan, C.G., Jackson, S.E., and Griffin, W.L., Data reduction software for LA-ICP-MS: appendix, in *LA-ICP-MS in the Earth Sciences: Principles and Applications*, Sylvester, P.J., Ed., *Mineral. Assoc. Can. Short Course Ser.*, 2001, vol. 29, pp. 239–243.

Vernikovsky, V.A., Pease, V.L., Vernikovskaya, A.E., Romanov, A.P., Gee, D.G., and Travin, A.V., First report of Early Triassic A-type granite and syenite intrusions from Taimyr: product of the northern Eurasian superplume? *Lithos*, 2003, vol. 66, nos. 1–2, pp. 23–36. https://doi.org/10.1016/S0024-4937(02)00192-5

Vernikovsky, V.A., Dobretsov, N.L., Metelkin, D.V., Matushkin, N.Yu., and Koulakov, I.Yu., Concerning tectonics and the tectonic evolution of the Arctic, *Russ. Geol. Geophys.*, 2013, vol. 54, no. 8, pp. 838–858. https://doi.org/10.1016/j.rgg.2013.07.006

Vernikovsky, V., Vernikovskaya, A., Proskurnin, V., Matushkin, N., Proskurnina, M., Kadilnikov, P., Larionov, A., and Travin, A., Late Paleozoic–Early Mesozoic granite magmatism on the Arctic margin of the Siberian Craton during the Kara–Siberia oblique collision and plume events, *Minerals*, 2020, vol. 10, no. 6. https://doi.org/10.3390/min10060571

Wiedenbeck, M.P.A., Corfu, F., Griffin, W.L., Meier, M., Oberli, F., von Quadt, A., Roddick, J.C., and Spiegel, W., Three natural zircon standards for U–Th–Pb, Lu–Hf, trace element and REE analyses, *Geostand. Geoanal. Res.*, 1995, vol. 19, pp. 1–23. https://doi.org/10.1111/j.1751-908X.1995.tb00147.x

Zhang, X., Pease, V., Carter, A., Kostuychenko, S., Suleymanov, A., and Scott, R., Timing of exhumation and deformation across the Taimyr fold-thrust belt: Insights from apatite fission track dating and balanced cross-sections, *Spec. Publ.—Geol. Soc. London*, 2018, vol. 460, no. 1, pp. 315–333. https://doi.org/10.1144/SP460.3

Translated by D. Voroshchuk